Jiang, Y., Su., M., and Chen, Q. 2003. "Using large eddy simulation to study airflows in and around buildings," *ASHRAE Transactions,* 109(2), 517-526.

# Using Large Eddy Simulation to Study Airflows in and around Buildings

Yi Jiang, Ph.D. ASHRAE Member
Mingde Su, Ph.D.
Qingyan Chen, Ph.D.* ASHRAE Member

ABSTRACT

This investigation uses three subgrid-scale models of large eddy simulation (LES) to study airflows in and around buildings. They are the Smagorinsky model, a filtered dynamic subgrid-scale model and a stimulated small-scale subgrid-scale model. For outdoor airflow that is highly turbulent, the simple Smagorinsky model is sufficient. For indoor airflow where laminar flow can be as important as turbulent one, the filtered dynamic subgrid-scale model and the stimulated small-scale subgrid-scale model are recommended. However, the computing time required by the filtered dynamic subgrid-scale model and the stimulated small-scale subgrid-scale model are considerably higher than that by the Smagorinsky model. This paper also discusses how to set up boundary conditions for wind and how to simulate indoor and outdoor airflow together with good resolution and reasonable size of computational domain for natural ventilation studies.

KEYWORDS: air flow, indoor air quality, modeling, turbulence, ventilation

## 1. INTRODUCTION

Study of airflows in and around buildings helps us understand the effectiveness and energy performance of ventilation systems, indoor air quality, thermal comfort, smoke dispersion, and fire development in buildings, pollution spread in urban area, and impact of wind load on building structure systems. The properties of building airflows, such as velocity, temperature, pressure, and species concentration, etc. are determined by supply air, thermal buoyancy, building geometry and spatial arrangements, and weather conditions. Correct prediction of building airflows is very challenging.

Measurements on a building site or in a full-scale environmental facility can provide reliable airflow distributions around and inside a building. Katayama et al. (1989), Fernandez and Bailey (1992), Dascalaki et al. (1995), and Yuan (1999) have performed such measurements. However, on-site measurements are time consuming and the measured data are normally with very low resolution so that they cannot be easily generalized. The experiment in a full-scale environmental facility is not only time consuming but also expensive. Furthermore, studies of airflow around a building often use wind tunnels that could simulate wind conditions. Notable studies of this type

* Yi Jiang was a Research Assistant at Massachusetts Institute of Technology and now is a Mechanical Engineer, RES Engineering Inc., Hudson, MA, Mingde Su were a Senior Post-Doctoral Associate at Massachusetts Institute of Technology is now with Chrysler, Detroit, MI and Qingyan Chen is a Professor, School of Mechanical Engineering, Purdue University, West Lafayette, IN.

Chen's phone: (765)496-7562, fax: (765)496-7534, email: yanchen@purdue.edu, and mailing address: 585 Purdue Mall, West Lafayette, IN 47907-2088

of airflow include those from Murakami et al. (1991) and Choiniere and Munroe (1994). With a wind tunnel, buildings are scaled down but the instrumentation used can disturb flow patterns and lead to accuracy problems (Murakami et al. 1991). With thermal buoyancy, scale models in a wind tunnel would have problem to simulate both inertial and buoyancy forces according to similarity theory.

Computational fluid dynamics (CFD) provides an alternative approach to obtain detailed airflow distributions in and around buildings. CFD is becoming popular due to its informative results and low labor and equipment costs, as a result of the development in turbulence modeling, and in computer graphics, speed and capacity. There are three different CFD methods: direct numerical simulation, Reynolds-averaged Navier-Stokes (RANS) modeling, and LES.

Direct numerical simulation solves the Navier-Stokes equation without approximations. The method requires the use of very fine grid resolutions to compute the smallest eddies in flow. To solve airflows in and around a building, DNS would require at least a grid number of $10^{11}$. Current super computers can handle a grid resolution as fine as $10^{8}$. In addition, it would take years of CPU time in a super computer to solve a meaningful problem of airflow in and around buildings. Therefore, the computer capacity is still far too small and the computer speed is far too slow with the direct numerical simulation method.

RANS modeling requires little computing time and is the most commonly used method to solve engineering airflows. To solve building airflows, however, RANS modeling has some key limitations. First, RANS modeling cannot accurately predict airflow around buildings. Lakehal and Rodi (1997) compared the computed results of airflow around a bluff body by using various RANS and LES models. They found that most RANS models had difficulties generating the separation region on the roof, which was observed in the experiment. Furthermore, the RANS models over-predict the recirculation region behind the body. On the other hand, the LES models did not encounter these problems, and their results agreed well with the experimental data. Secondly, the Reynolds stresses in the RANS method are unknown and have to be modeled with a turbulence model. Chen (1995) tested a number of popular turbulence models and concluded that none of them are universal for indoor airflow simulation. Building designers who are not very familiar with turbulence models have difficulties choosing a suitable model for the design of building airflow systems. On the contrary to the RANS models, the subgrid-scale models of LES are more universal because of the physics of the model development, which will be stressed below

LES method has been successfully used to solve building airflows in recent years (Davidson and Nielsen 1996, Emmerich and McGrattan 1998, Zhang and Chen 2000, Su et al. 2001, Jiang and Chen 2001, Jiang and Chen 2002, and Jiang et al. 2003). LES separates flow motions into large eddies and small eddies. The method computes the large eddies in a three-dimensional and time dependent way while it estimates the small eddies with a subgrid-scale model. When the grid size is sufficiently small, the impact of the subgrid-scale models on the flow motion is negligible. Furthermore, the subgrid-scale models tend to be universal because turbulent flow at very small scale seems to be isotropic. Therefore, the subgrid-scale models of LES generally contain only one or no empirical coefficient. Since the flow information obtained from subgrid scales may not be as important as that from large scales, LES can be a general and accurate tool to study engineering flows (Piomelli 1999, and Lesieur and Metais 1996). The building airflow in the current study is only a small portion of the atmospheric boundary layer (ABL). To simulate ABL turbulence, where the height of the layer is typically 1,000 meters, the grid size is much larger than a local integral turbulence scale in the near wall region. Therefore, a traditional

subgrid-scale model of LES needs to be modified to account the impacts of scale variations (Porte-Agel et al., 2000). Furthermore, the real ABL often contains abrupt changes of surface roughness and substantial transportations of eddies, heat, moisture and pollution vertically through the boundary layer. Since it is still unclear how the coherent structure is adjusted under those conditions, such a non-equilibrium simulation is not considered in the current investigation.

Hence, this paper will introduce the LES method and discuss the accuracy and demand for CPU time when it is applied to study airflows in and around buildings. The accuracy of LES is generally related to subgrid-scale models, while the computing time to the numerical techniques.

## 2. SUBGRID-SCALE MODELS OF LARGE EDDY SIMULATION

By filtering the Navier-Stokes and continuity equations, one would obtain the governing equations for the large-eddy motions as

$$\frac{\partial \overline{u_i}}{\partial t} + \frac{\partial}{\partial x_j}(\overline{u_i}\,\overline{u_j}) = -\frac{1}{\rho}\frac{\partial \overline{p}}{\partial x_i} + \nu \frac{\partial^2 \overline{u_i}}{\partial x_j \partial x_j} - \frac{\partial \tau_{ij}}{\partial x_j} \tag{1}$$

$$\frac{\partial \overline{u_i}}{\partial x_i} = 0 \tag{2}$$

where the bar represents grid filtering. The subgrid-scale Reynolds stresses, $\tau_{ij}$, in Equation (1),

$$\tau_{ij} = \overline{u_i u_j} - \overline{u}_i \overline{u}_j \tag{3}$$

are unknown and must be modeled with a subgrid-scale model.

Various subgrid-scale models have been developed in the past thirty years. Three of them are presented in this paper:

1. Smagorinsky subgrid-scale (SS) model (Smagorinsky 1963)
2. Filtered dynamic subgrid-scale (FDS) model (Zhang and Chen 2000)
3. Stimulated small-scale subgrid-scale (SSS) model (Shah and Ferziger 1995)

### 2.1 Smagorinsky Subgrid-Scale Model

The Smagorinsky subgrid-scale model (Smagorinsky 1963) is the simplest subgrid-scale model, and has been widely used since the pioneering work by Deardorff (1970). The SS model assumes that the subgrid-scale Reynolds stress, $\tau_{ij}$, is proportional to the strain rate tensor,

$$\overline{S}_{ij} = \frac{1}{2}\left(\frac{\partial \overline{u}_i}{\partial x_j} + \frac{\partial \overline{u}_j}{\partial x_i}\right) \tag{4}$$

$$\tau_{ij} = -2\upsilon_{SGS}\overline{S_{ij}} \tag{5}$$

where the subgrid-scale eddy viscosity, $\upsilon_{SGS}$, is defined as

$$\upsilon_{SGS} = (C_{SGS}\Delta)^2(2\overline{S_{ij}}\cdot\overline{S_{ij}})^{\frac{1}{2}} = C\Delta^2(2\overline{S_{ij}}\cdot\overline{S_{ij}})^{\frac{1}{2}} \quad (6)$$

The Smagorinsky constant, $C_{SGS}$ , ranges from 0.1 to 0.2 determined by flow types, and the model coefficient, C, is the square of $C_{SGS}$. The SS model is an adaptation of the mixing length model of RANS modeling to the subgrid-scale model of LES.

2.2 Filtered Dynamic Subgrid-Scale Model

The SS model requires a priori specification of the model coefficient, C, and a damping function must be used to account for near wall effects. It is difficult to specify the model coefficient in advance and the coefficient may not be a constant. In order to solve the problem, Germano et al. (1991) developed a subgrid-scale model with a dynamic procedure, which is usually called a dynamic model. This model can determine the coefficient as a function of time and location. The dynamic model has no prescribed coefficient, is physically sound, and therefore is very attractive.

The original dynamic model is computationally unstable. The least square approach provided by Lilly (1992) is widely adapted to stabilize the solution. The dynamic subgrid-scale model has the key features of proper asymptotic behavior near walls and the subgrid-scale eddy viscosity can vanish in the regions of laminar flow. However, this dynamic subgrid-scale model can still lead to numerical instability if the subgrid-scale eddy viscosity remains negative for too long. To overcome this difficulty, Germano et al. (1991) averaged the flow variables over a homogenous direction. For a channel flow, it is possible to identify the homogeneous direction. For airflows in buildings, there is no homogeneous direction. To stabilize the calculation, Zhang and Chen (2000) introduced a filtered dynamic subgrid-scale model. In the FDS model, a local average procedure replaces the average procedure over a homogeneous direction. This method is different from the local averaging procedure proposed by Zang et al. (1993). As pointed out by Zhang and Chen (2000), although Zang et al.'s (1993) method can effectively reduce the fluctuation for low-Reynolds number cavity flow, Zang et al.'s (1993) method does not work for indoor airflow that does not have a homogeneous direction. Therefore, we use the FDS model proposed by Zhang and Chen (2000).

The model coefficient, C, in the FDS model is calculated as follows:

$$C = \frac{\int G_f(\mathbf{x},\mathbf{x}')\,\overline{L}_{ij}\overline{M}_{ij}\,d\mathbf{x}'}{\int G_f(\mathbf{x},\mathbf{x}')\,\overline{M}_{ij}\overline{M}_{ij}\,d\mathbf{x}'} \quad (7)$$

where

$$L_{ij} = \widetilde{\overline{u}_i\overline{u}_j} - \widetilde{\overline{u}}_i\widetilde{\overline{u}}_j \quad (8)$$

$$M_{ij} = \alpha_{ij} - \widetilde{\beta}_{ij} \quad (9)$$

$$\alpha_{ij} = 2\widetilde{\overline{\Delta}}^2\left|\widetilde{\overline{S}}\right|\widetilde{\overline{S}}_{ij} \quad (10)$$

$$\beta_{ij} = 2\overline{\Delta}^2\left|\overline{S}\right|\overline{S}_{ij} \quad (11)$$

and ~ stands for an explicit test filter with a filter width of $\widetilde{\Delta}$ $(\widetilde{\Delta} = 2\overline{\Delta})$ and $G_f(\mathbf{x},\mathbf{x}')$ is a smooth function.

The C is obviously a function of time and space, and it can be applied to inhomogeneous flows. The smooth function $G_f(\mathbf{x},\mathbf{x}')$ should be chosen for the entire flow domain and may depend on the turbulent scales. Although the smooth function can be in many forms, a box filter may be the most convenient ($G_f(\mathbf{x},\mathbf{x}') = G(\mathbf{x},\mathbf{x}')$). Equation (7) indicates that C can be negative that implies the flow energy from small scales is transferred to the resolved large scales. However, the negative C can lead to numerical instability. In order to avoid the instability, the present investigation sets C = max (0.0, Equation (7)).

### 2.3 Stimulated Small-Scale Subgrid-Scale Model

Most of subgrid-scale models, such as the SS and FDS models, are eddy viscosity models, which apply Boussinesq hypothesis to calculate the eddy viscosity. A non-eddy viscosity model, named as stimulated small-scale subgrid-scale model, was developed by Shah and Ferziger (1995). This method attempts to obtain the unresolved parameters by using mathematical and/or physical methods based on statistical theory or DNS data, which is the reason to be called as "stimulated". The method applies successive inversion of a Taylor series expansion to represent the unknown full velocity in terms of the filtered velocity and this series expansion model is of scale-similarity form.

The SSS model calculates the subgrid stresses from

$$\tau_{ij} = \overline{u_i^* u_j^*} - \overline{u_i^*}\ \overline{u_j^*} \tag{12}$$

The SSS model expands variables, such as velocities, with Taylor series, so that the unknown subgrid-scale stresses can be computed.

$$u(x) = u_i^* + (x - x_i)\left(\frac{du}{dx}\right)_i^* + \frac{(x - x_i)^2}{2}\left(\frac{d^2u}{dx^2}\right)_i^* + \cdots\cdots \tag{13}$$

By neglecting the third-order and higher-order terms and replacing the derivatives with central differencing ones, this equation becomes

$$u(x) = u_i^* + (x - x_i)\frac{u_{i+1}^* - u_{i-1}^*}{2h} + \frac{(x - x_i)^2}{2}\frac{u_{i+1}^* - 2u_i^* + u_{i-1}^*}{h^2} \tag{14}$$

Su et al. (2001) gave a detailed mathematical explanation about this model.

## 3. NUMERICAL METHODS

This section discusses the numerical scheme employed for solving the governing equations with appropriate boundary conditions. Since this investigation involves natural ventilation, how to effectively calculate both indoor and outdoor airflows will also be addressed in this section.

### 3.1 Numerical schemes

With the subgrid-scale models, the present study uses the simplified marker and cell method (Harlow and Welch 1965) to solve the governing equations of LES. In order to correlate the momentum equation and the continuity equation, the simplified marker and cell method first

solves the momentum equations without the pressure term. So the velocity obtained, $\overline{u}_i^*$, is a pseudo-velocity.

$$\frac{\partial \overline{u}_i^*}{\partial t} + \frac{\partial}{\partial x_j}(\overline{u}_i \overline{u}_j) = \nu \frac{\partial^2 \overline{u}_i}{\partial x_j \partial x_j} - \frac{\partial \tau_{ij}}{\partial x_j} + g_j \beta(\overline{\theta} - \theta_0)\delta_{ij} \tag{15}$$

Subtracting Equation (1) from Equation (15) yields

$$\frac{\partial(\overline{u}_i^* - \overline{u}_i)}{\partial t} = \frac{1}{\rho}\frac{\partial p}{\partial x_i} \tag{16}$$

Then, by differentiating both sides of Equation (16) and using Equation (2), we have

$$\frac{\partial}{\partial t}\left(\frac{\partial \overline{u}_i^*}{\partial x_i}\right) = \frac{1}{\rho}\frac{\partial^2 p}{\partial x_i^{\,2}} \tag{17}$$

Equation (17) is a Poisson equation. This investigation applies a strong-implicit procedure (Stone 1968) or a fast Fourier transformation method to solve the Poisson equation. The fast Fourier transformation method requires less computing time than the strong-implicit method. But currently it requires a uniform grid distribution along at least one direction. This situation works for some building airflows. However, for most airflows around and inside buildings, the grids along all three directions are normally non-uniformly distributed due to the strongly inhomogeneous characteristics of the airflows and building geometry. Therefore, the fast Fourier transformation method needs to be further improved before being used as a general method to solve the Poisson equation.

### 3.2 Boundary Conditions

Boundary conditions, including the treatments of walls, and inflow and outflow conditions, are needed to close the equation. They are discussed in this section.

If a no-slip boundary condition is used for the airflows around and inside buildings, a large number of fine grids close to the walls are needed, which is not practical at present due to limitations on computer capacity. Therefore, a macroscopic boundary condition, a wall model, has to be introduced into the airflow study in buildings. The current study uses the wall model suggested by Werner and Wengle (1991). This model can be applied to both fully developed turbulent regions and regions of unsteady laminar flow, which are common in airflows around and inside buildings.

When applying LES to study airflow around buildings, the boundary conditions at open boundaries, which include inflow and outflow conditions, are complex due to the effects of up and down-stream obstacles, free stream turbulence, etc. The inflow conditions are with or without wind. For the situation without wind, there are no inertial forces to the open boundary and only buoyancy forces drive the air movement inside the computational domain. Therefore, a zero-gradient condition can be applied at the boundary. If the computational domain is large enough, a symmetrical or non-slip condition can also be adopted.

With wind, the technique for generating a realistic wind at the inflow boundary is very important. Two important issues have to be addressed in this wind simulation: the fluctuations of wind speed and wind direction. The simplest method to simulate wind fluctuation is to store the time history of velocity fluctuations given from a preliminary LES computation (Werner and Wengle 1991 and Shah 1998). However, this method requires extra computing costs to generate a series of transient flow fields and a large amount of memory to store the data. The current

study uses random fluctuations superimposed on a mean velocity profile at the inlet. The fluctuations are constructed to be of the same magnitude as the real wind. It is observed that wind direction changes over time and its histogram exhibits some rules (Nitta 1990). Following these rules, Jiang and Chen (2002) successfully used LES to simulate the directional fluctuation of wind around and across buildings.

The treatment of an outflow boundary condition is also important. The boundary condition at the exit should cause a minimal influence on the upstream and should permit eddies in the flow to exit the domain without any adverse effect on the flow field inside the computational domain. The current investigation uses the zero-gradient condition that has been used successfully for a long time.

### 3.3 Determination of Computational Domain

When using LES to study airflows both inside and outside of a building, such as natural ventilation, the computational domain must be large enough to capture macro-scale outdoor airflow and the grid resolution must be high enough to obtain detailed micro-scale indoor airflow. However, if the domain is too large, the computing time will be increased significantly. This is particularly true when Cartesian coordinate system is used. To save computing time while ensuring detailed indoor airflow information, it is better to separate indoor and outdoor calculations. When simulating macro-scale outdoor airflow, buildings can be treated as solid blocks without openings, such as windows. This is because the size of building openings is normally less than 1/6 of the total facade area and the effect of the openings on the outdoor airflow distributions can be neglected (Vickery and Karakatsanis 1987). The grid distribution in this outdoor flow simulation can therefore be relatively coarse so that a large computational domain can be covered. This would lead to an error of less than 5%. The separation of indoor and outdoor airflow calculations can reduce the computing time significantly and makes it possible to use LES to study a large-scale multi-building site.

## 4. RESULTS AND DISCUSSION

In this section, the subgrid-scale models of LES are used to study both indoor and outdoor airflows. The examples of indoor airflows are natural, forced, and mixed convection, which are common situations inside a building. The results are then compared with experimental data to evaluate the model performance.

### 4.1 Natural Convection in a Room

To study indoor airflow driven by buoyancy forces, the airflow circulated within a cold and a warm wall is investigated. Although this cavity type is not a real indoor condition, the airflow characteristics are very similar to those inside a room. Therefore, this case can be regarded as an indoor airflow driven by buoyancy forces. Detailed air velocity, temperature, turbulence energy, and heat transfer were measured by Cheesewright et al. (1986).

Figure 1 shows the airflow distributions along the middle height of the cavity. The RANS modeling with the standard k-ε model is also used as a comparison. The figure shows that the two subgrid-scale models gave good results for mean velocities and temperatures. However, the

SS model predicted much too small turbulence kinetic energy than the experimental data. The results computed with the FDS model were in better agreement with the experimental data.

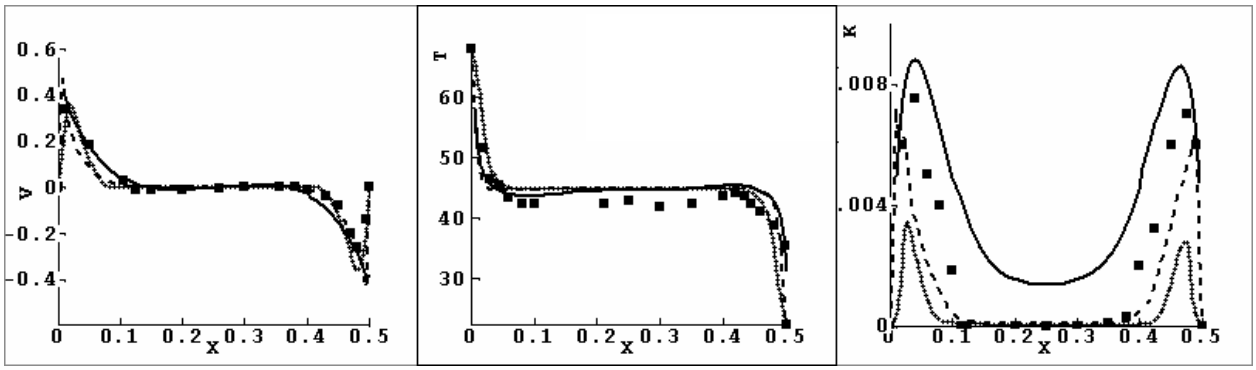


(a) Mean velocity (b) Mean temperature (c) Turbulence kinetic energy

*Figure 1. Comparison of the computed airflow distributions along the mid section of the walls with the experimental data (Cheesewright et a. 1986). Squares: Experiment, Solid lines: RANS modeling with the k-ε model, Dotted lines: SS model with $C_{SGS}$ = 0.16, Dashed lines: FDS model.*

4.2 Forced convection in a Room

The LES models have also been applied to study a forced convection flow in a room. The velocity was measured by Nielsen et al. (1978) with a laser Doppler anemometer. This case represents a simple but typical indoor ventilation situation. Figure 2 shows the computed airflow pattern in the mid-section. Besides a large recirculation in the center of the room, there is a small eddy in the upper right corner, which was also observed in the experiment. Figure 3 shows the comparison with measured data for the mean air velocity, represented by U, and the fluctuating air velocity, represented by ur. The FDS and SSS models perform slightly better than the SS model. This suggests that for indoor airflow cases, in which walls normally have significant effects and both turbulent and laminar flows exist, the SS model may not be appropriate.

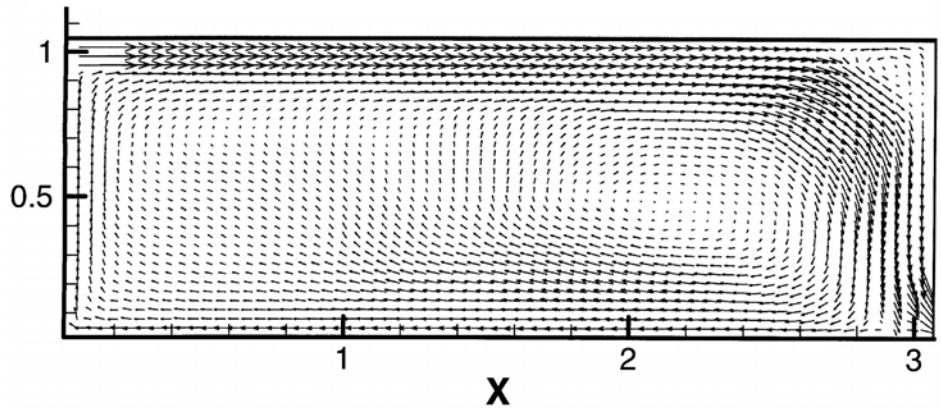


*Figure 2. The computed mean velocity in the middle section of the room (LES with SS model).*

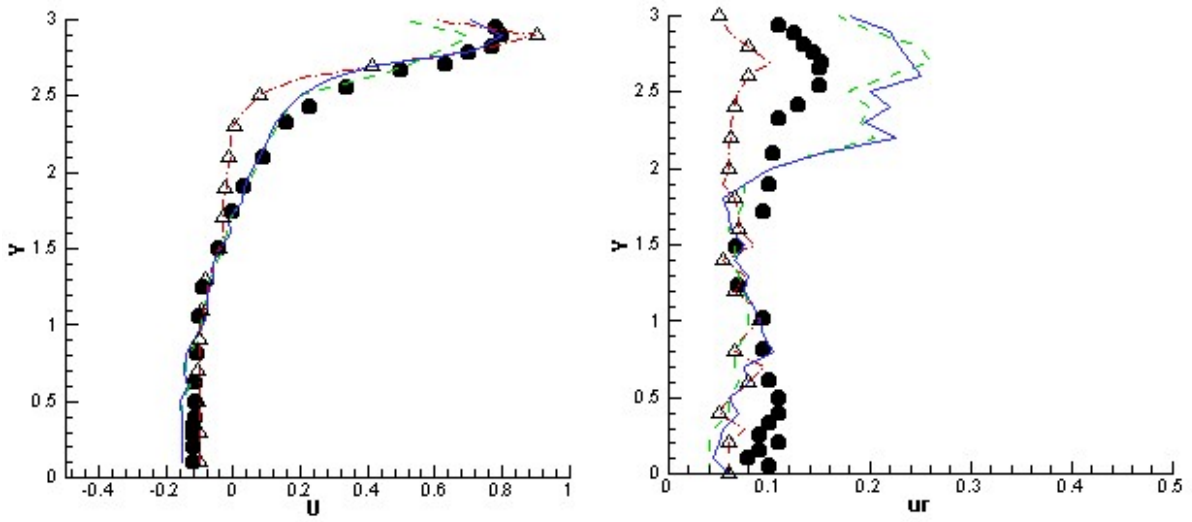


*Figure 3. Comparison of the computed mean and fluctuation velocity profiles with the experimental data (Nielsen et al. 1978) at x=1 section. Dots: experimental data, Triangles: SS model with 66x18x34 grids, Dot-dash lines: SS model with 66×34×34 grids, Dash lines: FDS model with 66×34×34 grids, Solid lines: SSS model with 66×34×34 grids.*

The distributions of the model coefficient, C, can show how the FDS model produces good results. Fig. 4 illustrates that C is small both near the walls and in the regions of laminar flow, which correctly represents the physics of flow motions.

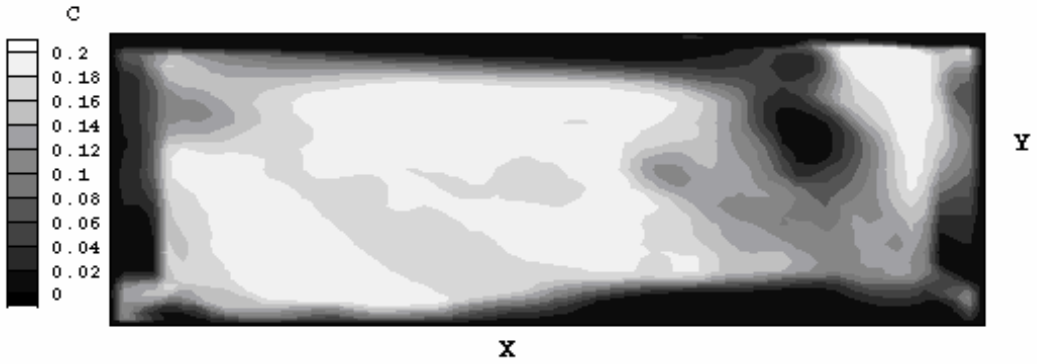


*Fig. 4. Distributions of the mean model coefficient, C, at the middle section of the room*

4.3 Mixed Convection in a Room

The mixed convection studied is the airflow in a room with displacement ventilation. Yuan et al. (1999) performed detailed experimental measurements on the distributions of air velocity, air temperature, and contaminant concentration by using a tracer-gas ($SF_6$). In the experiment, cool air was supplied through a diffuser in the lower part of a room and warm air was exhausted at the ceiling level. The room has two occupants, two PCs, overhead lighting, and furniture.

Figure 5 shows the mean airflow pattern in the mid-section of the room obtained with the SSS model of LES. Because of the buoyancy effect, the cold air from the diffuser moved rapidly downwards along the floor. The mean airflow pattern showed a large but weak recirculation in the lower part of the room. In the upper part of the room, there were some recirculations caused

by the thermal plumes from heated objects, such as PCs, occupants, and overhead lights. The computed airflow pattern was similar to that observed in the measurement. Figure 6 compares the computed mean air velocity, temperature, and $SF_6$ concentration with the experimental data in the center of the room. The results indicate that the three subgrid-scale models performed slightly different from each other. A model may work better than the others in one location but poorer in another.

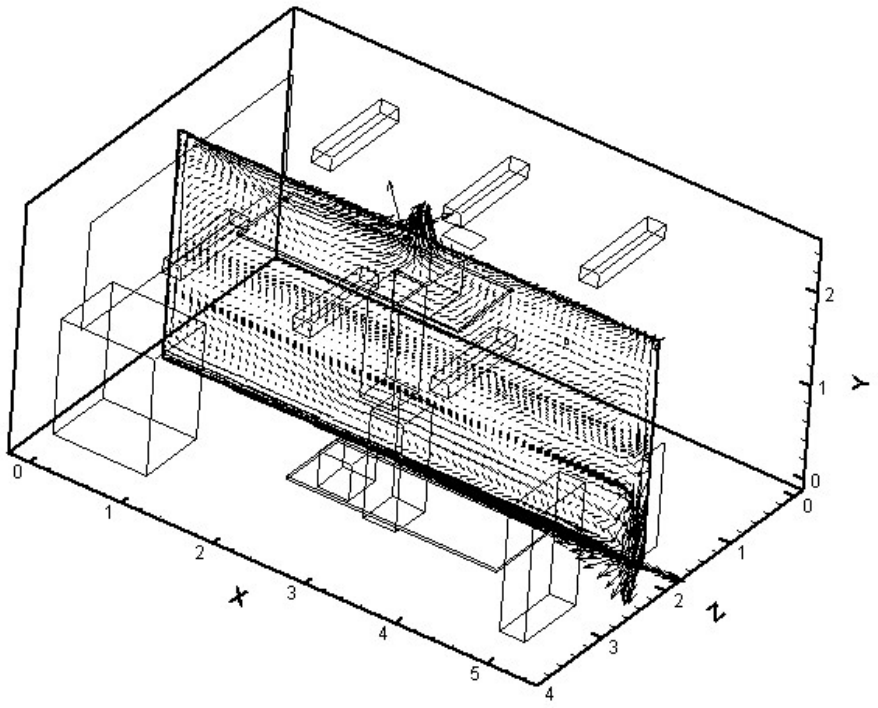


*Figure 5. The mean airflow pattern in the mid-section of the office (LES with SSS model).*

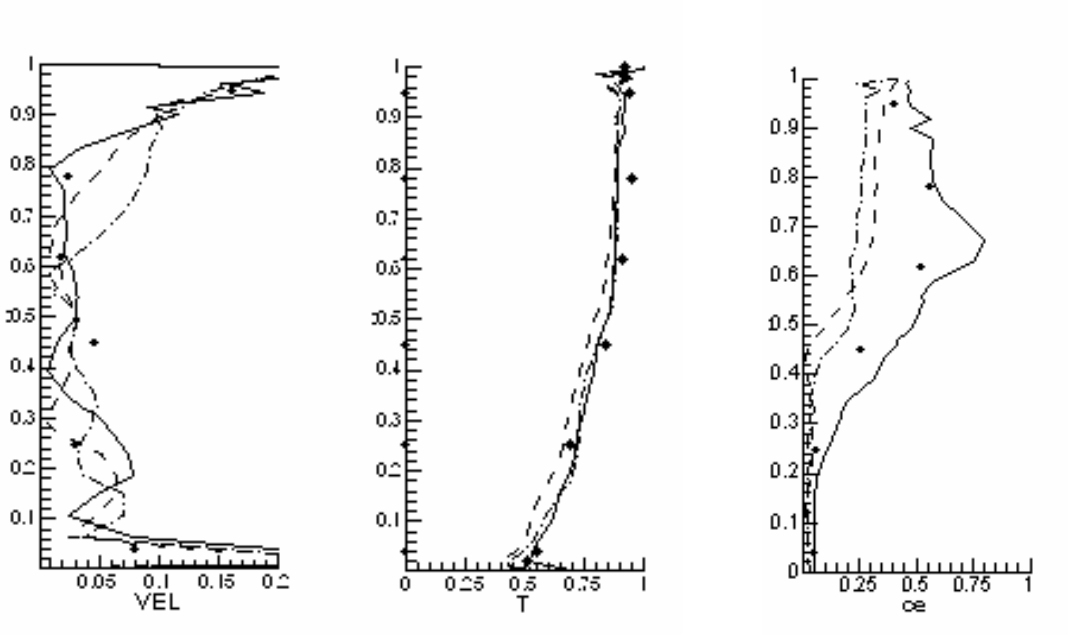


*Figure 6. Comparison of the computed profile of air velocity, temperature, and $SF_6$ concentration to the experimental data (Yuan et al. 1999) in the center of the room. The vertical coordinate is dimensionless room height, VEL is air velocity (m/s), T is normalized air temperature, and ce is normalized $SF_6$. ($ce=(c-c_s)/(-c_s)$, $c_s=0.42$ ppm, where $c_s$ is the tracer gas concentration at the source). Dots: experimental data, Dashed-dotted lines, SS model, Solid lines: FDS model, Dashed lines: SSS model.*

The performance of different subgrid-scale models to simulate indoor airflow can be summarized in Table 1. Please note that Reynolds numbers are computed based on the inlet height and inlet velocity and Rayleigh numbers are computed based on the temperature difference between the cold and the warm walls, the height of the walls and the distance between the two walls. It shows that in terms of accuracy, the SS performs fairly well in most regions as FDS and SSS model. The computing time required by the FDS model is 20% more than that by the SS model because it needs to calculate the coefficient C. Although it is mathematically sound, the SSS model needs twice as long computing time as the FDS model.

Table 1. Performance comparison with different subgrid-scale models of LES

| | Natural convection | | Forced convection | | | Mixed convection | | |
|---|---|---|---|---|---|---|---|---|
| | SS model | FDS model | SS model | FDS model | SSS model | SS model | FDS model | SSS model |
| Reynolds number | N/A | N/A | 5,000 | 5,000 | 5,000 | $10^4$ | $10^4$ | $10^4$ |
| Rayleigh number | $2.5x10^{10}$ | $2.5x10^{10}$ | N/A | N/A | N/A | N/A | N/A | N/A |
| Grid number | 69,192 | 69,192 | 99,200 | 99,200 | 99,200 | $10^5$ | $10^5$ | $10^5$ |
| Time step (second) | $2x10^{-4}$ | $2x10^{-4}$ | 0.06 | 0.06 | 0.06 | 0.005 | 0.005 | 0.005 |

| | | | | | | | | |
|---|---|---|---|---|---|---|---|---|
| Computing time (hours) [1] | 70 | 84 | 30 | 36 | 70 | 120 | 144 | 260 |
| 1st order Accuracy[2] | Good | Good | Fair | Good | Good | Good | Good | Good |
| 2nd order Accuracy[3] | Fair | Good | Fair | Fair | Fair | N/A | N/A | N/A |

[1]Computed on an Alpha workstation with a single 21264 processor
[2]Mean velocity, temperature, and contaminant concentration, etc.
[3]Turbulent kinetic energy, fluctuating velocity and temperature, etc.

4.4 Airflows in and around a Building

The SS and FDS models have been further applied to calculate airflow in and around a building for a natural ventilation study. This study also used a wind tunnel to measure detailed airflow around and within a simple, cubic, building-like model. Two-dimensional mean and fluctuating velocity components were measured by using a laser Doppler anemometer. The pressure distributions along the model surface were also measured. The Reynolds number studied is $1.4\times10^5$ based on the velocity at the building height in the inlet of the computational domain. Both of a coarse mesh, $100 \times 65 \times 80$, and a fine mesh, $140 \times 80 \times 110$, were used. It was found that the computed results with the coarse mesh are generally in good agreement with the experimental data. For example, the distributions of the mean and fluctuating velocities close to building openings were properly predicted with the coarse mesh and the ventilation rate can be calculated correctly. Therefore, to study natural, the coarse mesh is adopted. However, to investigate the flow distribution in some special regions, such as above the building roof, the fine mesh provided better results than the coarse mesh.

For the coarse mesh, the corresponding CPU time used is 150 hours for the SS model and 190 hours for the FDS model. For the fine mesh, the CPU time is more than three times longer than that required by the coarse grid due to the increased grid number and reduced time step size.

The measurements were conducted for several cases, such as the building has an opening in the windward direction, in the leeward direction, in the sidewalls, etc. LES has been used to simulate all of those cases. Here, the measured and computed velocities in single-sided ventilation with an opening in leeward wall are presented. Figure 7 shows the locations where the computed results from LES are compared with the measured data. Figure 8 shows that the mean velocities computed from LES are generally in good agreement with the experimental data. The difference between the experimental data and the LES results is less than 5% in most regions. This indicates that LES can be used to study wind-driven airflows around and within a building with excellent accuracy.

Figure 8 also illustrates that the results from both SS model and FDS model are almost the same. By analyzing the magnitudes of different terms in the momentum equation, we found that the contribution of the subgrid-scale stresses to the main flow motion is much smaller than that of the resolved (large-scale) stresses in most regions around the block. Therefore, most energy is contained in the large eddies, which play a more important role than the small eddies. Since both the SS and FDS models can directly solve the large-eddy motions, they are able to provide accurate flow results. In the current study, although the building model is not a blockage, most of the airflows outside of the building model are fully or nearly fully developed turbulent flows,

which are very similar to the airflows around a blockage. Hence, the computational results from the two subgrid-scale models are almost the same in most of the flow domain.

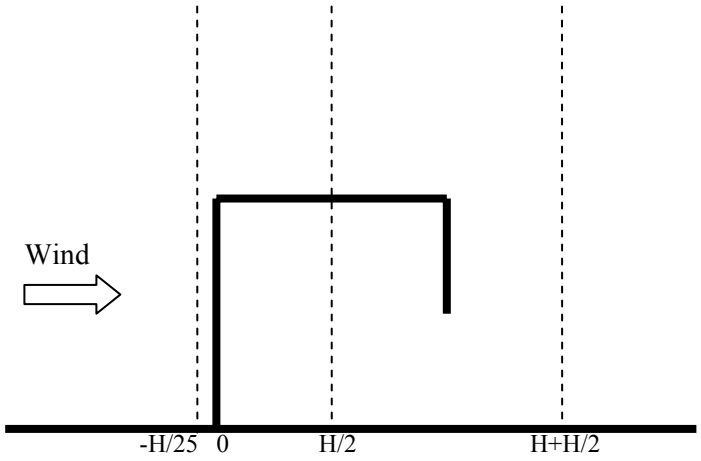


*Figure 7. The location where comparison of the LES results with experimental data was made in the mid-section (The thick lines represent the building model and the ground).*

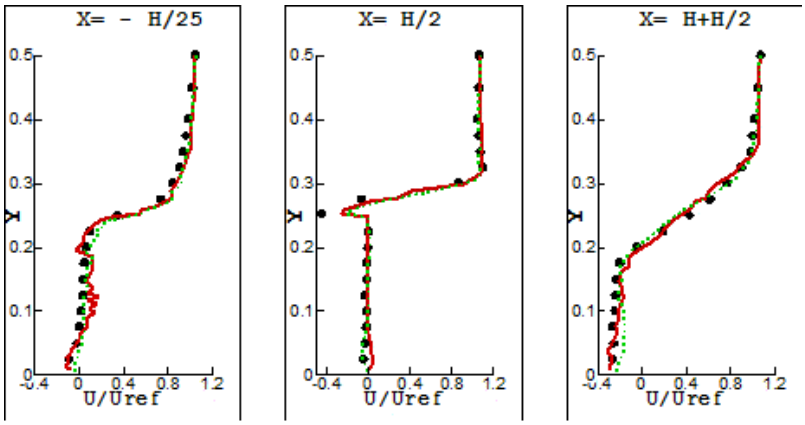


*(a) Mean velocity distributions*

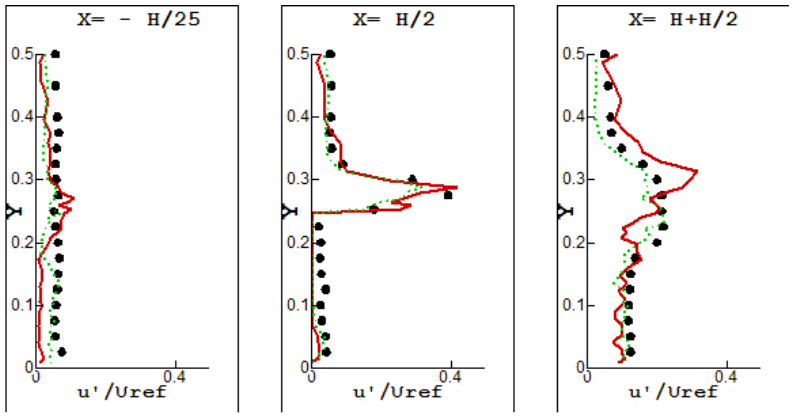


*(b) Fluctuating velocity distributions*

*Figure 8. Comparison of LES results of mean and fluctuation air velocity in horizontal direction for single-sided, leeward ventilation. Dots: experimental data; Solid line: SS model; Dotted line: FDS model. ($U_{ref}$ is the reference velocity at the building height and 2H in front of the building.)*

## 5. CONCLUSIONS

Three subgrid-scale models of LES have been used to study airflows in and around buildings. For outdoor airflow cases, the SS model works fairly well since the flows are fully turbulent. For cases where laminar phenomenon is as important as turbulent one, such as indoor airflows, the SS model performs poorly in some regions and the FDS and SSS models can give a much better result. Although the SSS model is mathematically sounded, it requires longer computing time than the other two models. Therefore, the SS model is recommended for outdoor airflow and FDS or SSS model for indoor airflow and combined indoor and outdoor airflows. When applying LES to study natural ventilation, it is better to separate the indoor airflow and outdoor airflow simulations. The separation helps to ensure that the computational domain is sufficiently large to accurately simulate upstream conditions and the grid resolution for indoor airflow is sufficiently fine to obtain detailed flow information.

## ACKNOWLEDGMENTS

This work is supported by the U.S. National Science Foundation under grant CMS-9877118.

## NOMENCLATURE

| | | | |
|---|---|---|---|
| C | model coefficient | $S_{ij}$ | strain rate tensor (1/s) |
| $C_{SGS}$ | Smagorinsky model constant | t | time (s) |
| $G_f$ | smooth function | $\vec{u}$ | air velocity (m/s) |
| h | grid size | $u_i$, $u_j$ | air velocity components in the $x_i$ |
| H | building height (m) | | and $x_j$ directions (m/s) |
| $L_{ij}$ | $= \widetilde{\overline{u}_i \overline{u}_j} - \widetilde{\overline{u}}_i \widetilde{\overline{u}}_j$ | $u^*$ | u at $x_i$ |
| $M_{ij}$ | $= \alpha_{ij} - \widetilde{\beta}_{ij}$ | $\overline{u}_i^*$ | pseudo-velocity |
| p | air pressure (Pa) | $x_i$, $x_j$ | coordinates in i and j directions (m) |
| Greek Symbols | | | |
| $\alpha_{ij}$ | $= 2\widetilde{\overline{\Delta}}^2 \left\|\widetilde{\overline{S}}\right\| \widetilde{\overline{S}}_{ij}$ | $\nu_{SGS}$ | subgrid-scale eddy viscosity ($m^2/s$) |
| $\beta_{ij}$ | $= 2\overline{\Delta}^2 \left\|\overline{S}\right\| \overline{S}_{ij}$ | $\rho$ | air density ($kg/m^3$) |
| $\Delta_i$ | filter width (m) | $\rho_p$ | particle density ($kg/m^3$) |

| | | | |
|---|---|---|---|
| $\nu$ | air kinematic viscosity ($m^2/s$) | $\tau_{ij}$ | subgrid-scale Reynolds stresses ($m^2/s^2$) |

REFERENCES


Cheesewright, R., King, K.J., and Ziai, S. Experimental data for the validation of computer codes for the prediction of two-dimensional buoyant cavity flows. HTD-60, ASME Winter Annual Meeting, Anaheim, December, 1986, pp. 75.

Chen, Q. 1995. Comparison of different k-ε models for indoor airflow computations, Numerical Heat Transfer, Part B: Fundamentals, 28, 353-369.

Choiniere, Y. and Munroe, J.A. 1994. A wind-tunnel study of wind direction effects on air-flow patterns in naturally ventilated swine buildings. Canadian Agricultural Engineering, 36 (2), 93-101.

Dascalaki, E., Santamouris, M., Argiriou, A., Helmis, C., Asimakopoulos, D., Papadopoulos, K. and Soilemes, A. 1995. Predicting single sided natural ventilation rates in buildings. Solar Energy 55 (5), 327-341.

Davidson, L. and Nielsen, P. Large eddy simulation of the flow in a three-dimensional ventilation room. 5th International Conference on Air Distribution in Rooms, ROOMVENT'96, July 17-19, 1996.

Deardorff, J. W. 1970. A numerical study of three-dimensional turbulent channel flow at large Reynolds numbers. Journal of Fluid Mechanics, 41, 453-480.

Emmerich, S.J. and McGrattan, K.B. 1998. Application of a large eddy simulation model to study room airflow. ASHRAE Transactions 104, 1128-1140.

Fernandez, J.E. and Bailey, B.J. 1992. Measurement and prediction of greenhouse ventilation rates. Agricultural and Forest Meteorology, 58 (3-4), 229-245.

Germano, M., Piomelli, U., Moin, P., and Cabot, W. H. 1991. A dynamic subgrid-scale eddy viscosity model. Physics of Fluids, A 3 (7), 1760-1765.

Harlow F. H. and Welch, J. E. 1965. Numerical calculation of time-dependent viscous incompressible flow. Physics of Fluids, 8 (12), 2182-2189.

Jiang, Y., Alexander, D., Jenkins, H., Arthur, R. and Chen, Q. 2003. Natural ventilation in buildings: Measurement in a wind tunnel and numerical simulation with large eddy simulation. Journal of Wind Engineering and Industrial Aerodynamics, 91(3), 331-353.

Jiang, Y. and Chen, Q. 2002. Study of cross natural ventilation in a building site by large eddy simulation. Building and Environment, 37, 379-386.

Jiang, Y. and Chen, Q. 2001. Study of natural ventilation in buildings by large eddy simulation. Journal of Wind Engineering and Industrial Aerodynamics, 89 (13), 1155-1178.

Katayama, T. Tsutsumi, J. Ishii, A. Nishida, M. and Hashida, M. 1989. Observations of heat flux in an urban area with a large pond by kytoons. Journal of Wind Engineering and Industrial Aerodynamics, 32, 41-50.

Lakehal, D., and Rodi, W. 1997. Calculation of the flow past a surface-mounted cube with two-layer turbulence models. Journal of Wind Engineering and Industrial Aerodynamics, 67 & 68, 65-78.

Lesieur, M., and Metais, O. 1996. New trends in large eddy simulations of turbulence. Annual Review of Fluid Mech., 28, 45-82.

Lilly, D.K. 1992. A proposed modification of Germano subgrid-scale closure method. Physics of Fluids A 4 (3), 633-635.

Murakami, S., Kato, S., Akabayashi, S., Mizutani, K. and Kim, Y.D. 1991. Wind tunnel test on velocity-pressure field of cross-ventilation with open windows. ASHRAE Transactions 97 part 1, 525-538.

Nielsen, P.V., Restivo, A. and Whitelaw, J.H. 1978. The velocity characteristics of ventilated room. Journal of Fluids Engineering, 100, 291-298.

Nitta K. 1990/1991. Cross-correlation between speed and direction of urban wind fluctuation. Energy and Buildings 15-16, 357-363.

Piomelli, U. 1999. Large Eddy simulation: achievements and challenges. Progress in Aerospace Sciences, 35, 335-362.

Piomelli, U., Cabot, W. H., Moin, P., and Lee, S., 1991, Subgrid-scale backscatter in turbulent and transitional flows. Physics of Fluids A 3, 1766.

Porte-Agel, F., Meneveau, C., and Parlange, M., 2000, A scale-dependent dynamic model for large-eddy simulation: application to a neutral atmospheric boundary layer. Journal of Fluid Mechanics, 415, 261-284.

Shah, K. B. 1998. Large eddy simulations of flow past a cubic obstacle. Ph.D. dissertation, Department of Mechanical Engineering, Stanford University.

Shah, K.B. and Ferziger, J.H. 1995. A new non-eddy viscosity sub-grid-scale model and its application to channel flow, Center for Turbulence Research. NASA Ames/Stanford University. Annual Research Briefs.

Smagorinsky, J. 1963. General circulation experiments with the primitive equations. I. The basic experiment. Monthly Weather Review, 91, 99-164.

Stone, H. L. 1968. Iterative solution of implicit approximations of multidimensional partial differential equations. SIAM Journal of Numerical Analysis, 5 (3), 530-558.

Su, M., Chen, Q., and Chiang, C.-M. 2001. Comparison of different subgrid-scale models and numerical schemes of large eddy simulation for indoor airflow modeling. Journal of Fluids Engineering, 123, 628-639.

Vickery, B.J., and Karakatsanis, C. 1987. External pressure distributions and induced internal ventilation flow in low-rise industrial and domestic structures. ASHRAE Transactions, 98(2), 2198-2213.

Werner, H., and Wengle, H. Large eddy simulation of turbulent flow over and around a cube in a plate channel. Eighth Symposium on Turbulent Shear Flows. Technical University Munich, September 9-11, 1991, 155-168.

Yuan, X., Chen, Q., Glicksman, L.R., Hu, Y., and X. Yang. 1999. Measurements and computations of room airflow with displacement ventilation, ASHRAE Transactions, 105(1), 340-352.

Zang, Y., Street, R. L., and Koseff, J. R., 1993, A dynamic mixed subgrid-scale model and its application to recalculating flow, Physics of Fluids, A 5, 3186-3195.

Zhang, W. and Chen, Q. 2000. Large eddy simulation of natural and mixed convection airflow indoors with two simple filtered dynamic subgrid scale models, Numerical Heat Transfer, Part A: Applications, 37(5), 447-463.